



# A novel donor–acceptor molecule containing a cyclic triphenylamine dimer: synthesis, characterization, and application in memory device

Yun Zhao<sup>a,b</sup>, Changqing Ye<sup>a,b</sup>, Yali Qiao<sup>a,b</sup>, Wei Xu<sup>b,\*</sup>, Yanlin Song<sup>b,\*</sup>, Daoben Zhu<sup>b,\*</sup>

<sup>a</sup> Beijing National Laboratory for Molecular Sciences, Organic Solids Laboratory, Institute of Chemistry, Chinese Academy of Sciences, Beijing 100190, PR China

<sup>b</sup> Graduate School of Chinese Academy of Sciences, Beijing 100049, PR China

## ARTICLE INFO

### Article history:

Received 18 October 2011

Received in revised form 23 November 2011

Accepted 2 December 2011

Available online 8 December 2011

## ABSTRACT

A novel highly soluble push–pull molecule containing electron-rich cyclic triphenylamine dimer (**TPAD**) and electron-poor *N*-phenyl-*N'*-octyl-naphthalene-1,4,5,8-tetracarboxylic acid bisimide [**NI-(8,PBr)**] was synthesized under Suzuki-coupling conditions. The resulting compound exhibited excellent thermal stability ( $T_d=354.3$  °C) and good solubility in common organic solvents. Cyclic voltammogram and optical absorption spectroscopy showed that both the electroactive units preserve their nature, respectively, in the ground state, whereas photophysical investigations showed a strong fluorescence quenching. Interestingly, excellent switching behavior with extremely high ON/OFF current ratio (1.6E8 at +1 V) was observed through memory devices based on thin films of this material.

© 2011 Elsevier Ltd. All rights reserved.

## 1. Introduction

During the last decade, organic electronic devices have been demonstrated to be promising candidates for inorganic-dominated electronic and optoelectronic devices, such as light emitting diodes,<sup>1,2</sup> solar cells,<sup>3</sup> and transistors.<sup>4</sup> Unlike the conventional inorganic semiconductor integrated circuits, which have to face the problem of scaling down in feature size,<sup>5,6</sup> the organic semiconductors have showed obvious advantages of rich structure flexibility, easy and low-cost fabrication, solution processability, and three dimensional stacking capability.<sup>7–10</sup>

Among all the organic materials, triphenylamine derivatives, due to their outstanding thermal stability, mechanical property, and electron-donating ability, have become more and more important in organic optoelectronic field. And the naphthalene diimides have also been thoroughly investigated for its electron-accepting ability, good planarity, and semiconducting properties.<sup>11</sup> In this study, a novel donor–accepter (D–A) molecule containing cyclic triphenylamine dimer and naphthalene diimides was synthesized and characterized. In the **TPAD** motif, the  $\pi$ -electron subsystems were placed in close proximity<sup>12</sup> and linked through vinylene bridge, which would extend the effective  $\pi$ -conjugation length, reduce the HOMO–LUMO energy gap, and tune the electrical properties.<sup>12,13</sup> Employing this novel molecule, an electronic

switching device was fabricated based on the solution-cast film, sandwiched between the indium–tin oxide (ITO) and Al electrodes. The device exhibited nonvolatile electrical switching and fulfilled the requirements of a write-once read-many times (WORM) memory device.

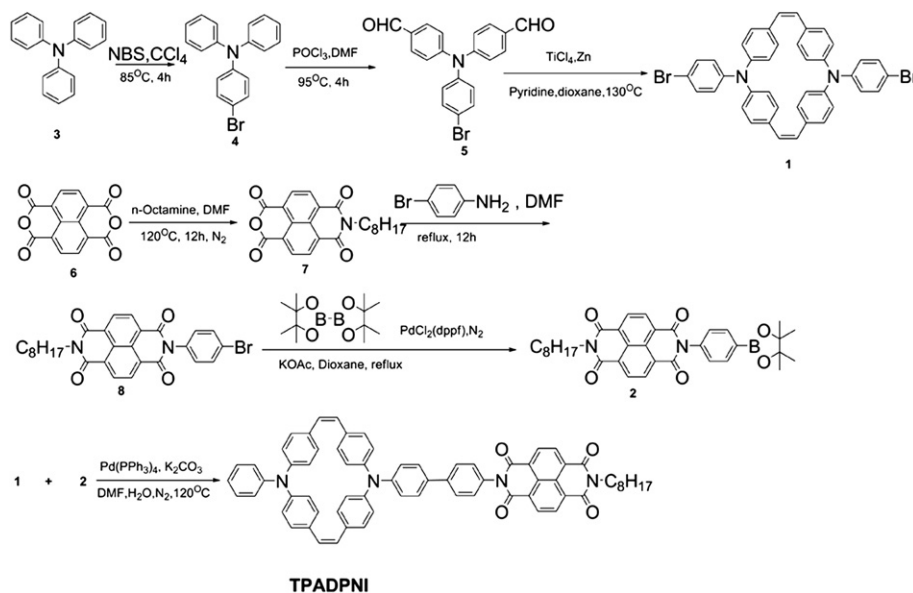
## 2. Results and discussion

The synthetic route of the desired molecule in this study was showed in **Scheme 1**. It was carried out by Suzuki coupling reaction between *N,N'*-diphenyl-4-bromoaniline dimer (**1**) and *N*-[4-(4,4,5,5-tetramethyl-1,3,2-dioxaborolan-2-yl)phenyl]-*N'*-octyl-naphthalene-1,4,5,8-tetracarboxylic acid (**2**). In this reaction, the solvent played a very important role on the final yield. Here, we chose DMF to accomplish the reaction, since subtle product can be obtained when toluene or 1,4-dioxane was used. Although a dibromo-substituted intermediate was employed, only one-substituted product could be isolated from the reaction mixture, the expected product with two naphthalene diimides units could just be detected in mass spectra. The bulk center part of compound **1** hindered the Suzuki coupling reaction and made the reaction very difficult to be accomplished, and one of bromine atom was eliminated in the transmetalation procedure.

### 2.1. Thermal properties

The thermal stability of **TPADPNI** sample was evaluated by thermogravimetric analysis (TGA) under a nitrogen atmosphere at a heating rate of 10 °C/min. The onset temperature of decomposition ( $T_d$ ) was determined to be 354.3 °C. The excellent

\* Corresponding authors. Tel.: +86 10 6263 9355; fax: +86 10 6256 9349 (W.X.); tel.: +86 10 6252 9284; fax: +86 10 82672719 (Y.S.); tel.: +86 10 6254 4083; fax: +86 10 6256 9349 (D.Z.); e-mail addresses: [zhaoyun@iccas.ac.cn](mailto:zhaoyun@iccas.ac.cn) (Y. Zhao), [wuxu@iccas.ac.cn](mailto:wuxu@iccas.ac.cn) (W. Xu), [yisong@iccas.ac.cn](mailto:yisong@iccas.ac.cn) (Y. Song), [zhudb@iccas.ac.cn](mailto:zhudb@iccas.ac.cn) (D. Zhu).



**Scheme 1.** Synthetic route to prepare the target compound **TPADPNI**.

thermal stability of this compound was expected to meet the requirement of heat resistance in the electronics industry.

## 2.2. Electrochemical properties

The electrochemical properties were investigated by cyclic voltammetry in a 0.1 M dry dichloromethane solution of tetra-*n*-butylammonium hexafluorophosphate (*n*-Bu<sub>4</sub>NPF<sub>6</sub>) under a nitrogen atmosphere. It was carried out in a conventional three-electrode cell using Pt button working electrode, a platinum wire counter electrode, and an Ag/AgCl reference electrode at room temperature. The **TPADPNI** exhibited the first oxidation and the first reduction potentials [ $E_{\text{red}}^{\text{first}}$  (onset)] at +0.62 V and −0.52 V (Fig. 1), respectively. Thus the HOMO and LUMO values were experimentally calculated by the onset potentials taking the known reference level for ferrocene, 4.8 eV below the vacuum level, according to the Eq. 1:<sup>14</sup>

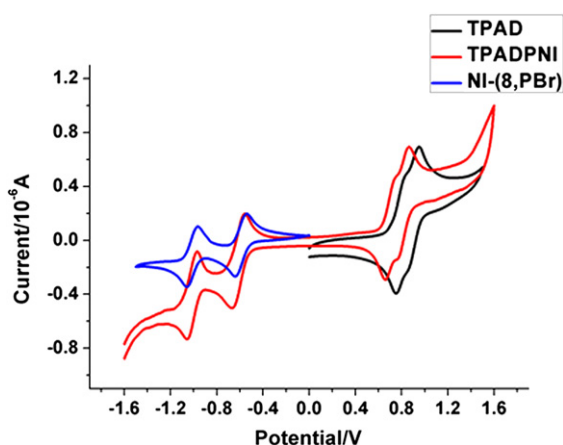


**Fig. 1.** Cyclic voltammogram measurement of **TPADPNI** and its constitutive units on a platinum working electrode in 0.1 M *n*-Bu<sub>4</sub>NPF<sub>6</sub>/CH<sub>2</sub>Cl<sub>2</sub> solution, with Ag/AgCl as the reference electrode and a platinum wire as the counter electrode. The concentration is  $\sim 1.0 \times 10^{-5}$  M.

$$\text{HOMO/LUMO} = -[E_{\text{onset}} - E_{\text{Ox}}(\text{ferrocene})] - 4.8 \text{ eV} \quad (1)$$

In the blank CV curve, the ferrocene exhibits an oxidation peak with an onset of 0.40 V versus Ag/AgCl. The calculated HOMO,

LUMO, and HOMO–LUMO energy bandgap values were −5.02 V, −3.88 V, and 1.14 V, respectively. The relatively low HOMO energy indicated good stability for its oxidation. Besides, the **TPAD** and the **NI-(8,PBr)** motifs showed separated oxidation and reduction peaks, respectively. This could be attributed to intramolecular electronic communication in each motif, and would reveal good stability of the initially formed radical cation.<sup>15</sup>

Since all potentials (vs Ag/AgCl) could be converted to values versus SCE by adding 0.29 V, the values of the ionization potential (IP) and the electron affinity (EA) could be also estimated from these onset potentials (vs SCE) using Eqs. 2 and 3:<sup>14</sup>

$$\text{IP} = E_{\text{first oxidation}} + 4.39 \text{ eV} \quad (2)$$

$$\text{EA} = E_{\text{first reduction}} + 4.39 \text{ eV} \quad (3)$$

where the constant 4.39 eV is the relationship between IP, EA, and the electrochemical potentials.<sup>16</sup> The IP and EA of **TPADPNI** were calculated to be 5.30 V and 4.16 V, respectively.

Also, we investigated the electrochemical behavior of its constitutive units, and found that the oxidation potentials of **TPADPNI** were very similar to those of donor motif. And so were the reduction potentials to those of acceptor motif. These indicated that the donor and acceptor moieties of **TPADPNI** had no significant charge transfer in the ground state.

## 2.3. Optical properties

The UV–vis absorption spectra of the **TPADPNI** together with those of donor motif (**TPAD**) and acceptor motif [**NI-(8,PBr)**] in diluted dichloromethane ( $1.0 \times 10^{-5}$  M) were shown in Fig. 2. The absorption spectrum of **TPADPNI** consisted on the approximate superposition of the absorption features of its constitutive units, and no new absorption bands were detected in **TPADPNI**. These confirmed that no significant interaction exists between the donor and acceptor motifs in the ground state, and were in agreement with the electrochemical behavior. The absorption spectrum of **TPADPNI** showed the characteristic bands arising from the acceptor motif between 230, 360, and 380 nm. And they were slightly affected by those of **TPAD** unit, which strengthened and blue-shifted the 360 nm band of **TPADPNI**. On the other hand, the 404 nm band of **TPAD** became quite obscure, which could be contributed to the small interaction with the acceptor motif. Also, the optical energy

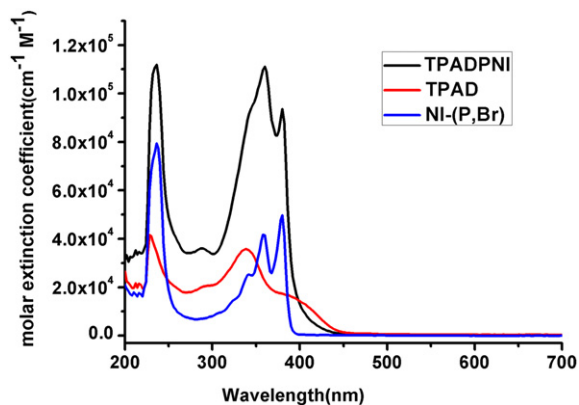


Fig. 2. UV-vis absorption spectrum of TPADPNI (dark line), TPAD (red line), and NI-(8,PBr) (blue line) in dilute dichloromethane solution.

gap derived from the absorption edge was 2.95 eV. Fluorescence emission spectra of TPADPNI and TPAD were measured in diluted dichloromethane solutions at fixed optical density using an excitation wavelength of 330 nm. Under this excitation, the stimulated TPAD showed very strong luminescence centered at 452 nm and 528 nm. However, the fluorescence properties of the TPADPNI, i.e., the TPAD motif, were greatly affected by the presence of the NDI motif. Thus, a quantitative quenching of the TPAD fluorescent emission was observed in compound TPADPNI in comparison with the fluorescence spectrum of TPAD (Fig. 3).

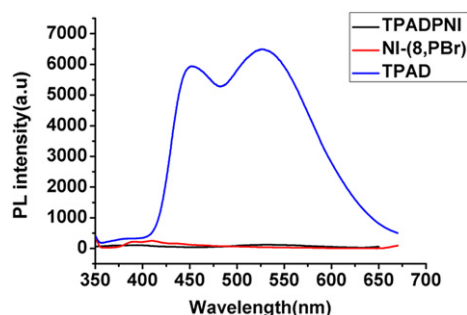


Fig. 3. Fluorescence spectrum of TPADPNI (black line), TPAD (blue line), and NI-(8,PBr) (red line) in diluted dichloromethane (1.0E-5 M).

The fluorescence quench can be explained by two ways. One is photoinduced energy transfer, the other is photoinduced electron transfer. Since there was little spectral overlap between the absorption spectrum of NI-(8,PBr) and the fluorescent spectra of the TPAD, the energy transfer from TPAD to NI-(8,PBr) will be prohibited due to the Förster mechanism.<sup>17</sup> Thus, we ascribe the fluorescence intensity quenching in compound TPADPNI to photoinduced electron transfer (PET) processes between the TPAD motif and the NI-(8,PBr) motif. And this is supported by the free energy  $\Delta G_{PET}$  of the corresponding photoinduced electron transfer process. According to the simplified Rehm–Weller relationship [Eq. 4], the  $\Delta G_{PET}$  is estimated to be  $-1.94$  eV.

$$\Delta G_{PET} = E_{D^+/D} - E_{A/A^-} - E_{00} \quad (4)$$

Here,  $E_{D^+/D}$  and  $E_{A/A^-}$  are the redox potentials of the electron donors and acceptor, respectively (0.73 and  $-1.09$  V, respectively).  $E_{00}$  is the energy of the excited state from which electron transfer occurs. As we all know, if  $\Delta G_{PET} < 0$ , electron transfer can occur from the photo-excited electron donor unit to the ground-state electron acceptor. If  $\Delta G_{PET} > 0$ , no photoinduced electron transfer can take place. However, time-resolved absorption spectra studies will be needed to provide further evidence for the above assumption.

## 2.4. Device fabrication and characterization

The TPADPNI (10 mg/ml) in the mix solution of chloroform and toluene was spin-coated onto a pre-cleaned indium–tin-oxide (ITO) glass. Aluminum top electrodes of  $0.2 \times 0.8$  mm<sup>2</sup> and 100 nm in thickness were thermally evaporated onto the organic molecular surface for the macroscopic memory devices. The electrical characteristics of the devices were characterized under ambient conditions, using a Keithley 4200-SCS semiconductor system and the Suss PM5 analytical probe station in a clean and shielded box under dark condition.

The sweep directions and typical current–voltage ( $I$ – $V$ ) characteristics of the ITO/TPADPNI (100 nm thick)/Al device were shown in Fig. 4. When a forward voltage was applied, the thin film exhibited a low-conductance state (OFF state, curve I). As the voltage approached  $+4.2$  V, a sharp increase in the current took place, indicating the thin film switched to a high-conductance state (ON state). After the transition, the thin film remained in the ON state during the second sweep from 0 to  $+10$  V (curve II). This OFF to ON transition can be viewed in a memory device as a ‘writing’ process. Once the device reached its ON state, it remained in this state, even after the power was turned off, or during the sequential forward voltage sweeping (curve II) and reverse voltage sweeping (curve III, IV). The nonvolatile and inert nature of the ON state suggests the TPADPNI device exhibits WORM type memory. The maximum ON/OFF current ratio could reach as high as  $1.6 \times 10^8$ . This extremely high value was very rare in the organic memory devices, and for all measured devices that were typically greater than  $10^6$ .<sup>18</sup> Such a high ON/OFF current ratio is crucial for the memory device to realize high-resolution and low-error-rate data storage.<sup>19</sup>

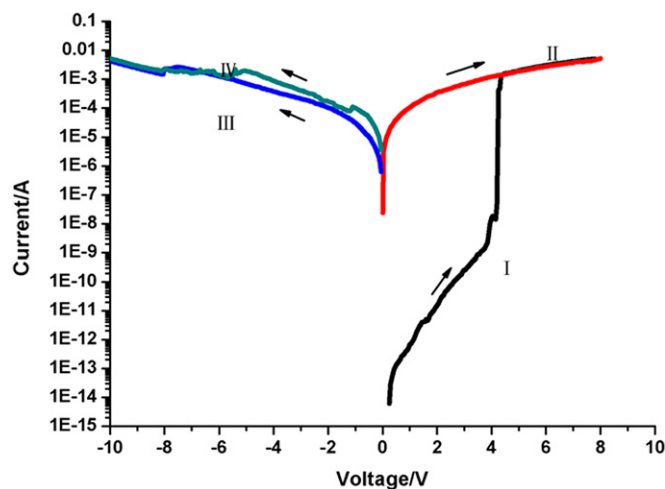


Fig. 4. Macroscopic  $I$ – $V$  characteristics of ITO/TPADPNI (100 nm thick)/Al.  $I_{on}$  (+1 V) =  $1.1E-4$ ,  $I_{off}$  (+1 V) =  $6.8E-13$ , the ON/OFF current ratio was  $1.6E8$ .

## 2.5. Proposed switching mechanism

To get a better understand of the switching behavior of the TPADPNI device, molecular calculations was carried out with the Gaussian 03 program package.<sup>20</sup> Equilibrium ground state geometry and electronic properties of basic unit of TPADPNI was optimized by means of the density functional theory (DFT) method at the B3LYP level of theory (Beckes-style three-parameter density functional theory using the Lee–Yang–Par correlation functional) with the 6-31 G(d,p) basic set. Fig. 5 shows the electron distribution of the HOMO and LUMOs, and the plausible electronic processes. Both the HOMO and LUMO3 isosurfaces tend to locate on the TPAD (D), while the LUMO and LUMO2 locate on the NI backbone (A). At the threshold voltage, electrons with sufficient energy transit from the

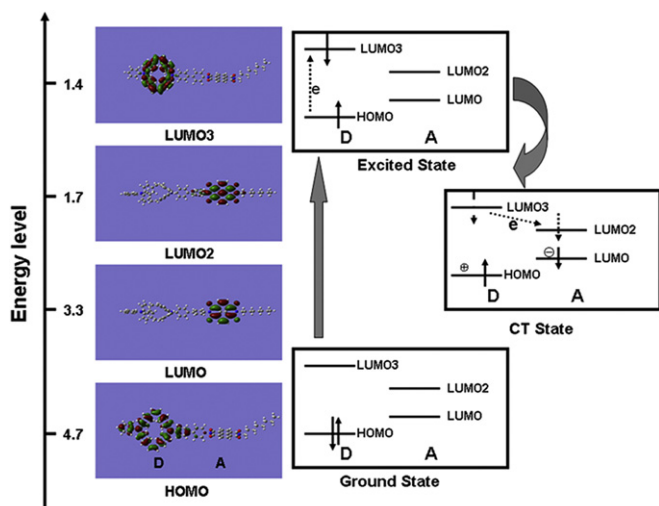


Fig. 5. Molecular orbitals (left) of TPADPNI and the transitions (right) from the ground state to the CT state induced by the electric field.

HOMO to the LUMO3 within D to form an excited state. Excitation of D leads to a decrease in ionization potential and consequently promotes intra- or intermolecular charge transfer (CT) at the excited state. CT can occur indirectly from the LUMO3 of D to the LUMO2, then to the LUMO of A, or directly from the HOMO to the LUMO2 and LUMO at the excited state, to form a conductive complex. This CT process is supported by the significant quenching of fluorescence in TPADPNI, as shown in Fig. 3. Under the electric field, the generated holes can delocalized among the TPAD donor moieties, generating an open channel for the charge carriers (holes) to migrate through. Thus, the current density increases rapidly to switch the device to the high-conductivity (ON) state. However, the intramolecular CT process is normally accompanied by a conformational change to more twisted conformation under the static electric field.<sup>21</sup> The twisted molecular chain can increase the potential energy barrier for the dissociation of CT complexes. As a result, the conductive CT state is stabilized and the high-conductivity (ON) state is retained. And this may well account for the stable ON state in Fig. 4.

### 3. Conclusion

This study reports the synthesis and characterization of a novel donor–acceptor molecule containing cyclic triphenylamine dimer and *N*-phenyl-*N'*-octyl-naphthalene-1,4,5,8-tetracarboxylic acid bisimide. This compound exhibits excellent thermal stability and good solubility in common solvents. Cyclic voltammetry and UV–vis spectroscopy shows that both electroactive units preserve their nature in the ground state, whereas photophysical investigations shows a strong fluorescence quenching, which makes this material a good candidate for the further investigation of the photophysical process. Meanwhile, the donor motif extends the conjugation and strengthened the good donating ability of triphenylamine, which makes it more favorable for organic electronics. Bistable electrical switching property is investigated through memory device, and an extremely high ON/OFF ratio (1.6E8) is observed. All of these performances indicate the newly synthesized material has great potential in photophysical, organic data storage and other electrical fields.

## 4. Experimental section

### 4.1. General procedures

All manipulations of air/moisture-sensitive materials were handled under nitrogen atmosphere using Schlenk techniques.

Dioxane was distilled over sodium/benzophenone. Pyridine was distilled over NaOH. All reagents were used as received unless otherwise noted. <sup>1</sup>H NMR and <sup>13</sup>C NMR spectra were obtained on Bruker Advance 400 or 600 spectrometers. EI-MS measurements were performed on UK GCT-Micromass or SHIMADZU G-MS-QP2010 spectrometers. High-resolution mass spectrometry measurements (HRMS) were performed on UK GCT-Micromass spectrometers. Elemental analyses were carried out on a Carlo Erba 1106 elemental analyzer.

4.1.1. *N,N*-Diphenyl-4-bromoaniline(**4**)<sup>22</sup>. Triphenylamine **3** (12.25 g, 50 mmol) and NBS (9.0 g, 50 mmol) were dissolved in 200 mL carbon tetrachloride. The solution was refluxed for 4 h. The precipitated succinimide was filtered, and the solvent was evaporated from the solution. The remaining gray oil was recrystallized from ethanol. The obtained white crystalline powder (14.4 g, 89%) was dried in a vacuum. Mp 102.6 °C, MS (EI): 323, 325. <sup>1</sup>H NMR (400 MHz, DMSO-*d*<sub>6</sub>) δ: 7.44–7.39 (m, 2H, H–Phe, *m* N); δ: 7.32–7.29 (m, 4H, H–Ph, *m* N); δ: 7.07–7.01 (m, 6H, H–Ph, *o* N, H–Phe, *o* N); δ: 6.90–6.88 (m, 2H, H–Ph, *p* N).

4.1.2. *N*-(4-bromophenyl)-*N,N*-bis(4-formylphenyl)-amine(**5**)<sup>23</sup>. POCl<sub>3</sub> (76.7 g, 500 mmol) was added dropwise to DMF (39 ml, 500 mmol) under a nitrogen atmosphere at 0 °C. The mixture was stirred for 1 h. Then **4** (6.48 g, 20 mmol) was added and the solution was stirred at 80 °C for 4 h. After cooling to room temperature, the resulting dark red suspension was washed with water and extracted with dichloromethane twice. The organic phase was dried over anhydrous sodium sulfate. The product was purified by column chromatography on silica gel using 4:1 petroleum ether/ethyl acetate as the eluent yielding an orange solid (4.64 g, 61%). Mp: 179.1 °C. MS (EI): 379, 381. <sup>1</sup>H NMR (400 MHz, DMSO-*d*<sub>6</sub>) δ: 9.89 (s, 2H); 7.86 (d, *J*=8.3 Hz, 4H); 7.63 (d, *J*=8.4 Hz, 2H); 7.22 (d, *J*=9.1 Hz, 4H); 7.16 (d, *J*=8.1 Hz, 2H). <sup>13</sup>C NMR (100 MHz, CDCl<sub>3</sub>) δ (ppm) 190.73, 151.90, 145.00, 133.58, 131.98, 131.72, 131.63, 130.52, 128.62, 127.40, 126.73, 123.34, 123.09, 119.51, 111.87.

4.1.3. *N,N*-diphenyl-4-bromoaniline dimmer (**1**)<sup>12,15</sup>. Zn powder (8.7 g, 132.8 mmol) was suspended in 200 ml dioxane under N<sub>2</sub>. TiCl<sub>4</sub> (14.4 ml) was added carefully to the suspension with stirring. Then the suspension was stirred at 120 °C for 1 h. A solution of **5** (1.25 g, 3.3 mmol) and pyridine (9 ml) in 100 ml dioxane was added dropwise to the reaction mixture. The mixture was stirred at 130 °C for 20 h. After cooling to room temperature, 200 ml saturated aqueous NaHCO<sub>3</sub> was added with stirring for 0.5 h. Then it was filtered, and the filtrate was extracted twice with dichloromethane (2×100 ml), and the combined organic extracts were dried over anhydrous sodium sulfate, filtered, and concentrated in vacuum. The residue was purified by chromatography on silica gel (dichloromethane/petroleum ether=4:1) to afford 468 mg (42% yield) of the desired product as yellow solid. Mp: >300 °C <sup>1</sup>H NMR (400 MHz, THF-*d*<sub>4</sub>) δ 7.18 (d, 4H, *J*=8.2 Hz, H–Phe, *o* Br); δ 6.88 (d, 8H, *J*=7.6 Hz, H–Phe, *o* Ethylene); δ 6.78–6.82 (m, 12H, H–Phe, *o* Br); δ 6.48 (s, 4H, H-Ethylene). <sup>13</sup>C NMR (100 MHz, THF-*d*<sub>4</sub>) δ (ppm) 147.96, 133.31, 132.15, 130.66, 130.38, 125.03, 123.29; HRMS (ESI): calcd for C<sub>40</sub>H<sub>28</sub>Br<sub>2</sub>N<sub>2</sub> 696.0599, found: 696.0606 (M<sup>+</sup>).

4.1.4. *N*-Octyl-naphthalene-1,8-dicarboxyanhydride-4,5-dicarboximide(**7**)<sup>24</sup>. 1,4,5,8-Naphthalenetetracarboxylic acid dianhydride (**6**) (5.0 g, 18.65 mmol) was refluxed under nitrogen with stirring in DMF (50 mL). A brownish slurry resulted. 1-Amino-octane (2.41 g, 18.65 mmol) was added dropwise down the condenser over 5 min. The reaction was refluxed for 15 h. After cooling to room temperature, the resulting dark suspension was washed with water and extracted with dichloromethane three times. The organic phase was dried over anhydrous sodium sulfate. The product was purified

by column chromatography on silica gel with dichloromethane to yield monoimide as white solid (1.893 g, 26.7%). Mp 181–183 °C, EI-MS (*m/z*): 379, <sup>1</sup>H NMR (400 M, CDCl<sub>3</sub>) δ 8.82 (s, 4H, H-Naphthalene rings); δ 4.20 (t, 2H, *J*=7.6 Hz, *N*-methylene); δ 1.43–1.28 (m, 12H, octyl chain); δ 0.88 (t, 3H, *J*=6.6 Hz, octyl chain methyl).

**4.1.5. *N*-(4-bromophenyl)-*N'*-octyl-naphthalene-1,4,5,8-tetracarboxylic acid bisimide(**8**)<sup>25</sup>.** Compound **7** (1.89 g, 5.0 mmol) and 4-bromoaniline (1.72 g, 10 mmol) were stirred under nitrogen in dry DMF (50 ml) at 130 °C for 12 h. When the solution was cooling down, it was washed with water and extracted with dichloromethane. The organic layer was dried over anhydrous sodium sulfate. The product was purified by column chromatography on silica gel with dichloromethane as eluent yielding 1.247 g yellow solid (46.9%). Mp 258–260 °C, <sup>1</sup>H NMR (400M, CDCl<sub>3</sub>): δ 8.77 (s, 4H, H-naphthalene rings); δ 7.70 (d, 2H, *J*=8.4 Hz, H–Phe, *o* N); δ 7.22 (d, *J*=8.4 Hz, H–Phe, *o* Br); δ 4.20 (t, 2H, *J*=7.6 Hz, *N*-methylene); δ 1.43–1.25 (m, 12H, H-octyl chain); δ 0.87 (t, 3H, *J*=6.3 Hz, H-octyl chain, methyl). <sup>13</sup>C NMR (100 MHz, CDCl<sub>3</sub>) δ (ppm) 163.07, 162.96, 133.89, 133.11, 131.74, 131.30, 130.58, 127.35, 127.12, 127.06, 126.78, 126.74, 123.63, 123.58, 41.41, 32.14, 32.11, 29.56, 28.40, 27.43, 22.96, 14.42; HRMS (EI): calcd for C<sub>28</sub>H<sub>25</sub>N<sub>2</sub>O<sub>4</sub>Br 534.0977 (100%), 532.0998 (98%), found: 534.0986 (100%), 532.1005 (98%).

**4.1.6. *N*-[4-(4,4,5,5-Tetramethyl-1,3,2-dioxaborolan-2-yl)phenyl]-*N'*-octyl-naphthalene-1,4,5,8-tetracarboxylic acid (**2**)<sup>26</sup>.** A solution of **8** (1.24 g, 2.33 mmol), bis(pinacolato)diboron (0.519 g, 2.71 mmol), **2**(dppf) (0.348 g, 0.42 mmol), and KOAc (0.67 g, 7 mmol) in dry 1,4-dioxane (15 ml) was stirred at 80 °C for 12 h under N<sub>2</sub>. After the solution was cooling down to room temperature, it was washed with water and extracted with dichloromethane twice. The organic layers were dried over anhydrous sodium sulfate. The product was purified by silica gel chromatography using 1% ethyl acetate in dichloromethane to give the target compound as white powder. (The product was easy to adsorb on the silica, so we treated the rough product with petroleum ether, and then filtered, the solid was used in the next step without further purification.) <sup>1</sup>H NMR: δ 8.78 (s, 4H, H-naphthalene rings); δ 8.03 (d, 2H, *J*=8.0 Hz, H–Phe, *o* N); δ 7.34 (d, 2H, *J*=8.0 Hz, H–Phe, *o* B); δ 4.2 (t, 2H, *J*=7.6 Hz, *N*-octyl methylene); δ 1.37 (m, 12H, 4CH<sub>3</sub>); δ 1.26 (m, 12H, H-octyl chain); δ 0.88 (t, 3H, *J*=6.0 Hz, H-octyl chain, methyl); MS(EI):580.

**4.1.7. TPADPNI<sup>26</sup>.** Compound **1** (696 mg, 1 mmol), compound **2** (1.6 g, 3 mmol), Pd(PPh<sub>3</sub>)<sub>4</sub> (124 mg, 0.1 mmol), and Cs<sub>2</sub>CO<sub>3</sub> (3.258 g, 10 mmol) were added to a 100 ml three necked Schlenk flask. Vacuum nitrogen cycles were repeated for three times. Then DMF (40 ml) and H<sub>2</sub>O were injected and the mixture was heated at 120 °C for 20 h. After the solution was cooling to room temperature, it was washed with water and extracted with dichloromethane twice. The organic layers were dried over anhydrous sodium sulfate, filtered and concentrated in vacuum. The residue was purified with silica gel chromatography yielding 246 mg pale yellow powder (24.8%). Mp: decomposing before melting. (*T*<sub>d</sub>=354.3 °C) <sup>1</sup>H NMR(600 M, CDCl<sub>3</sub>): δ 8.84–8.87 (d,d, 4H, H-naphthalene rings); δ 7.77 (d, 2H, *J*=8.3 Hz, H–Phe, *o* N-naphthalene); δ 7.53 (d, 2H, *J*=8.4 Hz, H–Phe, *m* N–2Phe); δ 7.39 (d, 2H, *J*=8.3 Hz, H–Phe, *m* N-naphthalene); δ 7.22 (t, 2H, *J*=7.9 Hz, H–Ph, *m* N); δ 7.16 (d, 2H, *J*=8.5 Hz, H–Phe, *m* N–2Phe); δ 7.06–7.09 (m, 6H, 2H–Ph, *o* N–2Phe; 4H–Phe, *o* N-Phe); δ 7.03 (d, 8H, *J*=7.6 Hz, *o* Ethylene);

δ 6.96–6.97 (m, 5H, 1H–Ph, *p* N; 4H–Phe, *m* Ethylene); δ 6.96 (s, 4H, H-ethylene); δ 4.24 (t, 2H, *J*=7.9 Hz, *N*-octyl methylene); δ 1.81 (t, 2H, H-octyl chain); δ 1.29 (m, 10H, H-octyl chain); δ 0.91 (t, 3H, *J*=9.2 Hz, H-octyl methane). <sup>13</sup>C NMR (150 M, CDCl<sub>3</sub>): δ (ppm) 163.24, 162.92, 148.23, 147.91, 146.79, 146.61, 141.86, 133.57, 133.49, 133.39, 132.92, 131.93, 131.55, 130.91, 130.84, 130.63, 129.53, 129.19, 128.37, 128.20, 127.53, 127.24, 125.61, 125.38, 122.17, 121.93, 41.56, 31.70, 29.80, 29.70, 28.63, 27.61, 23.15, 14.55. HRMS (ESI): calcd for C<sub>68</sub>H<sub>54</sub>N<sub>4</sub>O<sub>4</sub> 990.4145, Found 990.4140.

## Acknowledgements

This work was supported by Chinese Academy of Science.

## References and notes

- Tang, C. W.; Vanslyke, S. A. *Appl. Phys. Lett.* **1987**, *51*, 913–915.
- Friend, R. H.; Gymer, R. W.; Holmes, A. B.; Burroughes, J. H.; Marks, R. N.; Taliani, C.; Bradley, D. D. C.; Dos Santos, D. A.; Bredas, J. L.; Logdlund, M.; Salaneck, W. R. *Nature* **1999**, *397*, 121–128.
- Sariciftci, N. S.; Smilowitz, L.; Heeger, A. J.; Wudl, F. *Science* **1992**, *258*, 1474–1476.
- Gundlach, D. J.; Lin, Y. Y.; Jackson, T. N.; Nelson, S. F.; Schlom, D. G. *IEEE Electron Device Lett.* **1997**, *18*, 87–89.
- Reichmanis, E.; Katz, H.; Kloc, C.; Maliakal, A. *Bell Labs Tech. J.* **2005**, *10*, 87–105.
- Forrest, S. R. *Nature* **2004**, *428*, 911–918.
- Saxena, V.; Malhotra, B. D. *Curr. Appl. Phys.* **2003**, *3*, 293–305.
- Yang, Y.; Ouyang, J.; Ma, L. P.; Tseng, R. J. H.; Chu, C. W. *Adv. Funct. Mater.* **2006**, *16*, 1001–1014.
- Ling, Q. D.; Liaw, D. J.; Teo, E. Y. H.; Zhu, C. X.; Chan, D. S. H.; Kang, E. T.; Neoh, K. G. *Polymer* **2007**, *48*, 5182–5201.
- Mukherjee, B.; Pal, A. *J. Chem. Mater.* **2007**, *19*, 1382–1387.
- Doria, F.; di Antonio, M.; Benotti, M.; Verga, D.; Freccero, M. *J. Org. Chem.* **2009**, *74*, 8616–8625.
- Song, Y. B.; Di, C. A.; Yang, X. D.; Li, S. P.; Xu, W.; Liu, Y. Q.; Yang, L. M.; Shuai, Z. G.; Zhang, D. Q.; Zhu, D. B. *J. Am. Chem. Soc.* **2006**, *128*, 15940–15941.
- Roncali, J. *Chem. Rev.* **1997**, *97*, 173–205.
- Zhuang, X. D.; Chen, Y.; Li, B. X.; Ma, D. G.; Zhang, B.; Li, Y. X. *Chem. Mater.* **2010**, *22*, 4455–4461.
- Memminger, K.; Oeser, T.; Muller, T. J. *J. Org. Lett.* **2008**, *10*, 2797–2800.
- Miller, L. L.; Mayeda, E. A.; Nordblom, G. D. *J. Org. Chem.* **1972**, *37*, 916–918.
- Gomez, R.; Segura, J. L. *Tetrahedron* **2009**, *65*, 540–546.
- Ma, Y.; Cao, X. B.; Li, G.; Wen, Y. Q.; Yang, Y.; Wang, J. X.; Du, S. X.; Yang, L. M.; Gao, H. J.; Song, Y. L. *Adv. Funct. Mater.* **2010**, *20*, 803–810.
- Ling, Q. D.; Lim, S. L.; Song, Y.; Zhu, C. X.; Chan, D. S. H.; Kang, E. T.; Neoh, K. G. *Langmuir* **2007**, *23*, 312–319.
- Frisch, M. J.; Trucks, G. W.; Schlegel, H. B.; Scuseria, G. E.; Robb, M. A.; Cheeseman, J. R.; Montgomery, J. A., Jr.; Vreven, T.; Kudin, K. N.; Burant, J. C.; Millam, J. M.; Iyengar, S. S.; Tomasi, J.; Barone, V.; Mennucci, B.; Cossi, M.; Scalmani, G.; Rega, N.; Petersson, G. A.; Nakatsuji, H.; Hada, M.; Ehara, M.; Toyota, K.; Fukuda, R.; Hasegawa, J.; Ishida, M.; Nakajima, T.; Honda, Y.; Kitao, O.; Nakai, H.; Klene, M.; Li, X.; Knox, J. E.; Hratchian, H. P.; Cross, J. B.; Bakken, V.; Adamo, C.; Jaramillo, J.; Gomperts, R.; Stratmann, R. E.; Yazyev, O.; Austin, A. J.; Cammi, R.; Pomelli, C.; Ochterski, J. W.; Ayala, P. Y.; Morokuma, K.; Voth, G. A.; Salvador, P.; Dannenberg, J. J.; Zakrzewski, V. G.; Dapprich, S.; Daniels, A. D.; Strain, M. C.; Farkas, O.; Malick, D. K.; Rabuck, A. D.; Raghavachari, K.; Foresman, J. B.; Ortiz, J. V.; Cui, Q.; Baboul, A. G.; Clifford, S.; Cioslowski, J.; Stefanov, B. B.; Liu, G.; Liashenko, A.; Piskorz, P.; Komaromi, I.; Martin, R. L.; Fox, D. J.; Keith, T.; Al-Laham, M. A.; Peng, C. Y.; Nanayakkara, A.; Challacombe, M.; Gill, P. M. W.; Johnson, B.; Chen, W.; Wong, M. W.; Gonzalez, C.; Pople, J. A. *Gaussian 03, Revision B.04*; Gaussian: Wallingford, CT, 2004.
- Kang, E. T.; Liu, Y. L.; Wang, K. L.; Huang, G. S.; Zhu, C. X.; Tok, E. S.; Neoh, K. G. *Chem. Mater.* **2009**, *21*, 3391–3399.
- Bacher, E.; Bayerl, M.; Rudati, P.; Reckefuss, N.; Muller, C. D.; Meerholz, K.; Nuyken, O. *Macromolecules* **2005**, *38*, 1640–1647.
- Mallegol, T.; Gmouh, S.; Meziane, M. A. A.; Blanchard-Desce, M.; Mongin, O. *Synthesis-Stuttgart* **2005**, 1771–1774.
- Wiederrrecht, G. P.; Niemczyk, M. P.; Svec, W. A.; Wasielewski, M. R. *J. Am. Chem. Soc.* **1996**, *118*, 81–88.
- Chaignon, F.; Falkenstrom, M.; Karlsson, S.; Blart, E.; Odobel, F.; Hammarstrom, L. *Chem. Commun.* **2007**, 64–66.
- Sonar, P.; Singh, S. P.; Leclere, P.; Surin, M.; Lazzaroni, R.; Lin, T. T.; Dodabalapur, A.; Sellinger, A. *J. Mater. Chem.* **2009**, *19*, 3228–3237.